ACS APPLIED POLYMER MATERIALS

pubs.acs.org/acsapm

Article

Synthesis and Characterization of Homogeneous Epoxy Networks: Development of a Sustainable Material Platform Using Epoxy-Alcohol Polyaddition

Antonella Fantoni, Thomas Koch, Stefan Baudis,* and Robert Liska

Cite This: *ACS Appl. Polym. Mater.* 2023, 5, 731−742

Read Online

ACCESS | Metrics & More | Article Recommendations | Supporting Information

ABSTRACT: The development of bio-based epoxy resins from aliphatic biomass and lignin has rapidly increased over the past few decades. While thermal curing of such monomers with polyfunctional amines and anhydrides has been intensively discussed in literature, surprisingly, their polymerization behavior using alcohols as co-curing agents and the resulting mechanical properties have not been investigated in detail up to now. Herein, the polymerization mode of bio-based epoxides with alcohols using imidazoles as catalysts was studied *via* ^{1}H-NMR analysis, revealing a controlled alternating co-polymerization between difunctional epoxy and alcohol monomers. Furthermore, differential scanning calorimetry analysis was used to obtain the theoretical heat of polymerization (∼100 kJ mol^{-1}) of multifunctional monomers and the formulations exhibited high storage stabilities of up to 28 days. By varying the core structure and functionality of the epoxy monomers, high-performance thermosets with a tunable T_G (0−110 °C) and high tensile toughness of up to 18 MJ m^{-3} were obtained. These performances show potential for the application of bio-based epoxy networks as coatings for key industrial sections such as automotive technologies.

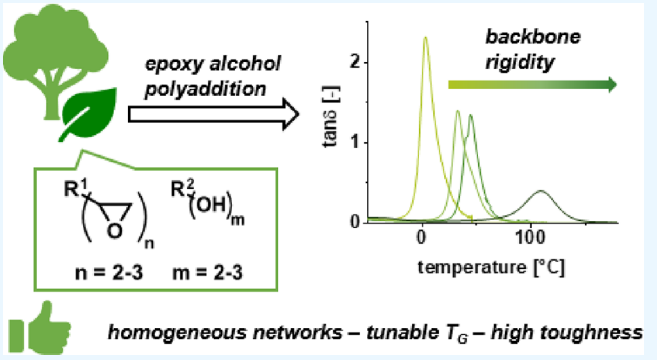

KEYWORDS: *bio-based epoxy monomers, vanillin, phloroglucinol, isosorbide, trimethylolpropane, sustainable polymers, polyaddition, imidazole*

INTRODUCTION

Epoxy resins represent one of the most important monomers for applications such as coatings, adhesives, casting formulations, or composites.[1,2] Due to their excellent thermomechanical properties including high glass transition temperatures (T_G), high glassy moduli (E') at 25 °C, and good chemical resistance,[1−3] polymers derived from epoxy monomers dominate the market of thermosets, making up roughly 70% of all thermosetting polymers.[3] These features enable the use of epoxy materials in civil infrastructures and automotive, aerospace, and aeronautical technologies.[4] Indeed, one of the biggest advantages of epoxy resins is their good performance at elevated temperatures owing to high glass transition temperatures. More precisely, T_G is of upmost importance for the design of materials for aeronautic industries as the materials should not experience softening in the operating temperatures (−50 to 60 °C). Therefore, T_G is expected to exceed the upper temperature limit, making high T_G polymers from renewable materials a hot topic in current research.[5]

Typically, epoxy monomers can be cured using co-curing agents comprising polyfunctional amines,[6] acids,[7] anhydrides,[8] phenols,[9] or thiols[10] at elevated temperatures. While the aforementioned co-curing agents polymerize in a step-growth manner with epoxides, tertiary amines, such as *N*,*N*-dimethylaniline or imidazoles, enable an anionic ring-opening polymerization of epoxides *via* chain growth. Furthermore, it is well known that tertiary amines act as accelerators in the epoxy-amine and epoxy-anhydride reaction.[11]

Indeed, imidazoles have attracted attention as curing agents due to their high reactivity in the anionic chain-growth polymerization of epoxy monomers.[12] The thermal curing of such monomers with 1-substitued and 1-unsubstituted imidazoles (Scheme 1) has been intensively studied over the past few decades.[13−15] Barton and Shepard proposed a two-step initiation mechanism for 1-unsubstitued imidazoles, where the more basic pyridine-type nitrogen attacks the oxirane ring and forms a (1:1) adduct. Rearrangement of the intermediate gives a second pyridine-type nitrogen that attacks another

Received: October 3, 2022
Accepted: November 28, 2022
Published: December 7, 2022

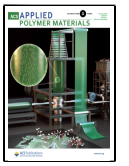

Scheme 1. Proposed Mechanisms for the Nucleophilic Attack[a]

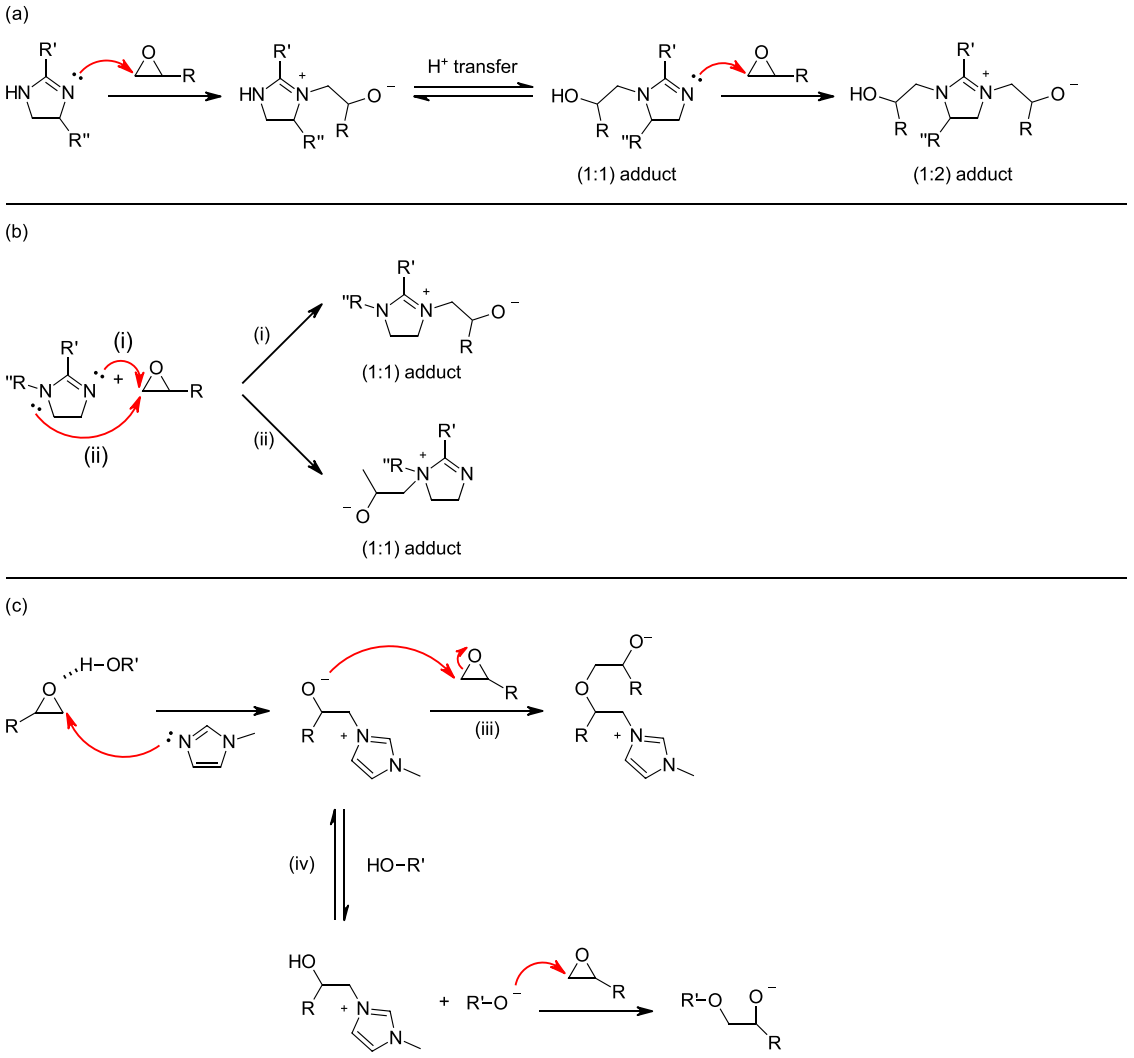

[a](a) 1-Unsubstituted and (b) 1-substituted imidazoles toward epoxy monomers with the formation of (1:1) and (1:2) adducts that initiate the polymerization *via* the alkoxide ion. (c) Possible mechanism of initiation of the anionic ring-opening polymerization of epoxides (iii) and chain transfer in the presence of hydroxyl groups (iv).[13−16]

epoxy group, giving the (1:2) adduct that eventually acts as the initiator (Scheme 1a). When 1-substituted imidazoles (such as 1-methyl imidazole) are used as initiators, two tertiary nitrogen atoms are present that can both initiate the attack on the epoxy ring to form the initiating (1:1) adduct (Scheme 1b).

Additionally, tertiary amines act as accelerators in epoxy-thiol click-reactions and epoxy-phenol and epoxy-alcohol polymerizations.[17,18] It is assumed that initiation occurs *via* the nucleophilic addition of the tertiary amine to the oxirane ring. However, Rozenberg showed that hydroxyl donating species such as alcohols or thiols participate in the initiation reaction.[19] Hydrogen bonding between the oxygen in the epoxide and the hydroxyl-containing species activates the oxirane species by an inductive effect. Subsequent deprotonation of −OH compounds results in the formation of alkoxide ions that may act as propagating sites in the progress of the reaction (Scheme 1c, pathway iv). Regarding imidazoles as catalysts, Foix *et al.* presented a possible mechanism for the chemical incorporation of hydroxyl groups into epoxy networks (Scheme 1c) using imidazole-type accelerators. The basicity of the imidazole enables the anionic polymerization of epoxides (Scheme 1c, pathway iii), while the presence of hydroxyl containing species leads to chain transfer. *Via* deprotonation of OH components, alkoxide anions are produced that may facilitate another ring-opening reaction of the epoxy monomers.[16]

Only a few reports of base-catalyzed epoxy-hydroxyl polymerizations and resulting networks were published in the last decade. Serra and co-workers described the tertiary amine- and imidazole-initiated reaction of epoxy resins with hydroxyl-terminated multiarm polymers and dendrimers in detail.[17,20,21] They showed that the conversion at the gel point was significantly increased in the presence of hydroxyl groups. Furthermore, hyperbranched additives led to increased toughness of the materials. Previous work by Kropka *et al.* focused on the reaction kinetics of epoxy monomers with diethanolamine as the hydroxyl donor.[22] With high concentrations of the hydroxyl components, proton transfer is possible and the alkoxide is transferred away from the polymer chain to small molecules (Scheme 1c, pathway iv), resulting in the formation of many small network clusters compared to few high molecular weight clusters in the anionic chain-growth

https://doi.org/10.1021/acsapm.2c01728
ACS Appl. Polym. Mater. 2023, 5, 731−742

Scheme 2. (a) Bio-Based Epoxy Monomers Trimethylolpropane Triglycidyl Ether (TMPTG), Epoxidized Isosorbide (ISE), Diglycidyl Ether of Vanillyl Alcohol (DGEVA), Epoxidized Phloroglucinol (PHTE), and the Multifunctional Alcohol Trimethylolpropane (TMP). (b) Tertiary Amines for the Catalyst Screening: *N,N*-Dmethylanilin (DMA), Imidazole (IM), 1-Methylimidazole (1MIM), Triethylamine (TEA), 1,5-Diazabicyclo[4.3.0]non-5-en (DBN), 1,1,3,3-Tetramethylguanidine (TMG), and Corresponding pK_a Values[35−37]

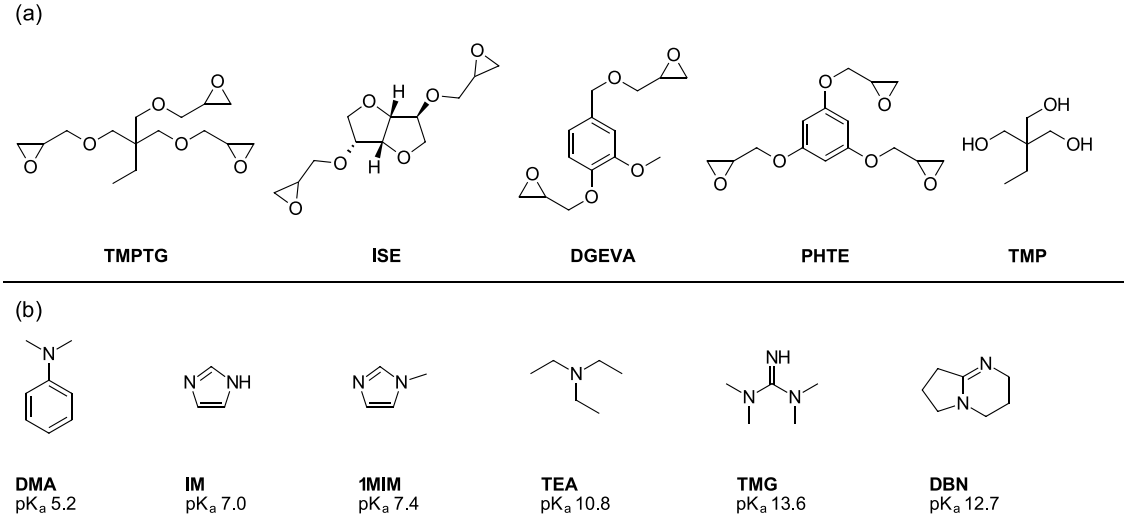

polymerization. The combination of many small clusters leads to a higher extent of curing at the gel point and a denser and more homogeneous network that is typical for step-growth reactions. However, they found that the polymerization mechanism (anionic chain growth vs step-growth-like proton transfer) and consequently the network structure are strongly temperature-dependent.

Regardless of their excellent thermomechanical properties, the majority of commercially available epoxy resins are produced from non-renewable, petrol-based chemicals, where the diglycidyl ether of bisphenol A (BADGE) dominates the industry.[3] However, bisphenol A is a known human endocrine disruptor, driving the search for alternative epoxy monomers that are both renewable and nontoxic.[3,23]

While intensive scientific research can be found on the thermal curing of bio-based epoxy monomers with polyfunctional amines and anhydrides,[3,24] very few data is reported about the thermal polymerization of such compounds in combination with alcohols and the underlying polymerization process. Herein, we present the thermal polymerization of sustainable epoxy monomers with a multifunctional alcohol as a co-curing agent (Scheme 2a) in a polyaddition reaction. While trimethylolpropane trigylcidyl ether (TMPTG) is a commonly used bio-derived reactive diluent,[25] epoxidized isosorbide (ISE) was chosen as it is considered to be a renewable alternative to BADGE.[26] Since Fache *et al.* and Stanzione *et al.* demonstrated that vanillin-derived epoxy networks demonstrate good (thermo)mechanical properties, the diglycidyl ether of vanillyl alcohol (DGEVA) was furthermore selected.[27−29] Additionally, it was decided to use the trigylcidyl ether of phloroglucinol (PHTE) as a trifunctional aromatic monomer from renewable resources since its trifunctional nature is known to increase the cross-linking density of the resulting polymers.[30] To ensure cross-linked networks in a polyaddition reaction, a multifunctional alcohol was chosen. While bio-based isosorbide, vanillyl alcohol, and phloroglucinol showed to be incompatible with the aforementioned epoxy monomers, trimethylolpropane (TMP) was the alcohol of choice. Tertiary amines are literature-known catalysts for the reaction of epoxides with hydroxyl donors.[16,19,20] Therefore, a catalyst screening was conducted first. Moreover, the reaction mechanism was investigated *via* a proton nuclear magnetic resonance (NMR) study and DSC measurements combined with Fourier transform infrared (FT-IR) highlighted the thermal reactivity and curing behavior. Furthermore, structure−property relationships of bio-based polymer networks were characterized using dynamic mechanical thermoanalysis and tensile tests. In view of potential high-end applications such as automotive, obtaining bio-based epoxy thermosets with good mechanical properties and variable glass transition temperatures, to ensure applicability of the material over a broad temperature range, was of upmost importance in this work.

EXPERIMENTAL SECTION

Materials and General Methods. The starting compounds isosorbide (TCI Europe), vanillyl alcohol, and phloroglucinol (TCI Europe) were purchased from the respective companies and used without further purification. Allyl bromide (TCI Europe), tetrabutylammonium bromide (TCI Europe), *m*-chloroperbenzoic acid (Sigma-Aldrich), epichlorohydrin (Sigma-Aldrich), tetrabutylammonium chloride (TCI Europe), sodium hydroxide (Merck), hexanediol (Sigma-Aldrich), trimethylolpropane (ACROS), resorcinol (Sigma-Aldrich), trimethylolpropane triglycidylether (Sigma-Aldrich), triethylamine (Sigma-Aldrich), dimethylaniline (Sigma-Aldrich), tetramethylguanidine (Fluka), diazabicyclo[4.3.0]non-5-en (Fluka), 1-methyl imidazole (Sigma-Aldrich), and imidazole (Fluka) were used without further purification. Commercial grade dichloromethane (CH_2Cl_2) was dried using a PureSolv system (inert).

Column Chromatography. Column chromatography was performed on a Büchi Sepacore flash system (Büchi pump module C-605, Büchi control unit C-620, Büchi UV-Photometer C-635, Büchi fraction collector C-660) using glass columns packed with silica gel (Merck).

NMR spectra. NMR spectra were recorded on a Bruker Avance DRX-400 FT-NMR spectrometer at 400 MHz for ^{1}H-NMR spectra and 100 MHz for ^{13}C-NMR spectra. The signals were reported with their chemical shifts in ppm and fine structure (s = singlet, d = doublet, t = triplet, q = quartet, qn = quintet, sep = septet, m = multiplet). The chemical shifts were referenced by using the

https://doi.org/10.1021/acsapm.2c01728
ACS Appl. Polym. Mater. 2023, 5, 731−742

respective NMR solvents [^{1}H: $CDCl_3$ (7.26 ppm), ^{13}C: $CDCl_3$ (77.16 ppm)] as internal reference.

Refractive Index. The refraction index n_D^{20} was measured with a Carl Zeiss Abbe refractometer with a Na lamp at 20 °C.

Melting Point. Melting points were measured on an OptiMelt automated melting point system from SRS (Stanford Research System). The heating rate was set to 1 °C min^{-1}.

Monomer Synthesis. *Synthesis of 4,8-Bis[(2-oxiranyl)-methoxy]-2,6-dioxabicyclo[3.3.0]octane (ISE).* The synthesis toward ISE was conducted in a modified two-step procedure by Chrysanthos *et al.*[26] by first preparing the intermediate diallyl isosorbide (ISAll), which was oxidized subsequently to ISE as described in the following chapters.

For the synthesis of ISAll, isosorbide (30.0 g, 205 mmol, 1 equiv) was mixed with NaOH (18.7 g, 452 mmol, 2.2 equiv) and 50 mL of water under vigorous stirring at room temperature. After 10 min, tetrabutylammonium bromide (2.98 g, 9.02 mmol, 0.05 equiv) was added as a phase transfer catalyst and the mixture was stirred for 5 min. Allyl bromide (40.0 mL, 452 mmol, 2.2 equiv) was added dropwise, and the mixture was thereafter heated to 70 °C for 7 h followed by stirring at room temperature for 16 h. The biphasic mixture was washed three times with 80 mL of CH_2Cl_2. Combined organic layers were washed with 200 mL of 1 N aq. HCl and 3 × 80 mL of H_2O and dried over sodium sulfate. The solvent was removed *in vacuo*, yielding 34.72 g (75% of theory) of a turbid crude oil that was directly used for the second step of the reaction.

n_D^{20}: 1.4845.

^{1}H-NMR (400 MHz, $CDCl_3$): δ 6.01−5.81 (m, 2H), 5.29 (d, 2H), 5.22−5.18 (d, 2H), 4.63 (t, 1H), 4.51 (d, 1H), 4.20 (m, 1H), 4.04−3.90 (m, 8H), 3.63−3.57 (m, 1H).

^{13}C-NMR (100 MHz, $CDCl_3$): δ 134.7/134.3, 118.0/117.6, 86.5, 83.9, 80.4, 79.6, 73.6, 71.8, 70.7, 70.0.

Subsequently, for the synthesis of ISE, *m*-CPBA (70% in H_2O, 28.1 g, 114 mmol) was dissolved in 160 mL of dry CH_2Cl_2 and cooled to 0 °C. Afterward, ISAll (11.7 g, 52.0 mmol, 1 equiv) was dissolved in 65 mL of CH_2Cl_2 and added to the cooled solution over the course of 2 h. After 1 h of stirring, a white precipitate was formed and the suspension was stirred for another 18 h. The reaction mixture was cooled to 0 °C and filtrated. The precipitate was washed two times with cold CH_2Cl_2, and the filtrate was washed with sat. aq. $Na_2S_2O_3$ (2 × 100 mL), sat. aq. $NaHCO_3$ (3 × 200 mL), and water (200 mL). Combined aq. layers were washed with CH_2Cl_2 (2 × 150 mL), pooled organic extracts were dried over Na_2SO_4, the solvent was stripped, and the light-yellow crude oil was further purified *via* column chromatography (petroleum ether:ethyl acetate = 1:9), yielding 8.31 g (65% of theory) of the desired product.

n_D^{20}: 1.4860.

^{1}H-NMR (400 MHz, $CDCl_3$): δ 4.67 (m, 1H), 4.52 (m, 1H), 4.16−3.36 (m, 10H), 3.24−3.09 (m, 2H), 2.84−2.76 (m, 2H), 2.67−2.55 (m, 2H).

^{13}C-NMR (100 MHz, $CDCl_3$): δ 86.3, 85.1, 80.6, 80.4, 73.6, 72.0, 70.5−70.0, 50.7, 44.5.

Synthesis of 2-[(2-Methoxy-4-{[(2-oxiranyl)methoxy]methyl}-phenoxy)methyl]-xirane (DGEVA). The synthesis was conducted according to a modified procedure by Fache *et al.*[27] The reaction was conducted in an inert atmosphere. Vanillyl alcohol (9.98 g, 65.0 mmol, 1 equiv) was stirred with epichlorohydrin (51 mL, 650 mmol, 10 equiv) and tetrabutylammonium chloride (1.52 g, 6.12 mmol, 0.1 equiv) at room temperature for 4 h using a mechanical stirrer. The clear pink solution was cooled to 0 °C with an ice bath, and an aqueous solution of NaOH (33 wt %, 38.9 g, 973 mmol, 15 equiv) was added dropwise over 30 min. The ice bath was left to melt over time, and the white suspension was stirred for 18 h. Thereafter, 250 mL of deionized water was added and the aqueous layer was washed three times with 200 mL of ethyl acetate. Pooled organic extracts were washed with water (100 mL) and brine (100 mL) and consequently dried over Na_2SO_4 and dried *in vacuo*. After purification *via* column chromatography (petroleum ether:ethyl acetate = 1:3), the desired compound was obtained as a white solid (14.23 g, 82% of theory).

m.p.: 52.7−53.1 °C (lit.: 53 °C[27]).

^{1}H-NMR (400 MHz, $CDCl_3$): δ 6.95−6.82 (m, 3H), 4.52 (d, 2H), 4.24 (dd, 1H), 4.04 (dd, 1H), 3.88 (s, 3H), 3.76 (dd, 1H), 3.42−3.34 (m, 2H), 3.19 (m, 1H), 2.89 (m, 1H), 2.81 (dd, 1H), 2.74 (dd, 1H), 2.61 (m, 1H).

^{13}C-NMR (100 MHz, $CDCl_3$, δ, ppm): 149.9, 147.8, 131.8, 120.5, 114.1, 111.8, 73.3, 70.8, 70.5, 56.1, 51.0, 50.3, 45.1, 44.4.

Synthesis of 2-({3,5-Bis[(2-oxiranyl)methoxy]phenoxy}methyl)-oxirane (PHTE). PHTE was synthesized in a modified procedure by Guzmán *et al.*[31] Phloroglucinol (10.3 g, 83.1 mmol, 1 equiv) was dissolved in epichlorohydrin (147 g, 1580 mmol, 19 equiv), tetrabutylammonium chloride (2.65 g, 12.3 mmol, 0.14 equiv) was added, and the reaction mixture was heated to 100 °C and stirred mechanically for 4 h. After cooling to 20 °C, NaOH (20.0 g, 500 mmol, 6 equiv) was added as a 20 wt % aqueous solution over 30 min. The suspension was stirred for 90 min at room temperature. After the addition of 60 mL of ethyl acetate, the phases were separated and the organic layer was washed with water (50 mL) and brine (2 × 50 mL) and dried over Na_2SO_4. The solvent was removed *in vacuo*, giving a yellow crude oil, which was purified *via* column chromatography (petroleum ether:ethyl acetate = 1:3), giving the desired compound as a white solid (12.6 g, 52% of theory).

m.p.: 53.1−53.8 °C (lit.: 53 °C[31]).

^{1}H-NMR (400 MHz, $CDCl_3$, δ, ppm): 6.14 (s, 3H), 4.18 (dd, 3H), 3.89 (dd, 3H), 3.26 (m, 3H) 2.90 (dd, 3H), 2.74 (dd, 3H).

^{13}C-NMR (100 MHz, $CDCl_3$, δ, ppm): 160.5, 94.8, 69.0, 50.2, 44.8.

Formulation and Specimen Preparation. For the investigation of suitable catalytic systems, TMPTG was used as the epoxy and TMP as the alcohol component. Formulations of around 1 g were prepared as follows: equimolar ratios of functional groups of TMPTG and TMP were weighed into glass vials and placed in a water bath (60 °C) to obtain homogeneous mixtures. After the catalyst (in 1−10 wt %) was added, the liquid mixture was mixed and degassed for 5 min in an ultrasonic bath. Thereafter, the liquid mixtures were poured into silicon molds (sticks, 5 × 2 × 40 mm^3) and cured, as depicted in the Supporting Information, Table S1.

For the imidazole screening, formulations of ∼1 g were prepared from TMPTG and TMP, maintaining an equimolar ratio of epoxy and alcohol reactive groups. Imidazole (0.1−10 wt %) was used as the catalyst. The preparation of polymer specimens was conducted as mentioned previously, and the samples were cured for 18 h at 90 °C.

For the proton NMR study, storage stability study, DSC, DMTA, and tensile test measurement formulations were prepared using 1 wt % of imidazole as the catalyst. The formulations were heated to 60 °C and homogenized using a vortex mixer. For the DSC measurement and proton NMR study, all formulations were directly used after preparation. For (thermo)mechanical measurements, the monomer formulations were casted in silicone molds (sticks, 5 × 2 × 40 mm^3 for DMTA; dog bone-shaped samples in accordance with ISO 527 test specimen 5b, a total length of 35 mm, and a parallel region of 2 × 2 × 2 mm^3 for tensile tests) at 90 °C for 18 h. The polymer specimens were ground to obtain uniform specimens with exact dimensions (deviations ≤ ±0.1 mm).

Catalyst Screening and FT-IR Spectroscopy. The conversion of the polymerization was determined by FT-IR spectroscopy by analysis of the change of the integral of the epoxy ring vibration signal (915 cm^{-1}) in reference to the integral of the aromatic ring vibration (800 cm^{-1}) for the monomers DGEVA and PHTE.[32] For the cycloaliphatic monomer ISE, the −C−H bending vibration (1460 cm^{-1})[26] and for the aliphatic monomer TMPTG the −C−H stretching vibration (2900 cm^{-1})[33] were used as references. Formulations were measured directly after preparation and after the polymerization on a PerkinElmer Spectrum 65 FT-IR spectrometer using a Specac MKII golden gate single reflection ATR system. The epoxy group conversion was calculated in eq 1

$$\text{epoxy group conversion [\%]} = \left(1 - \frac{\frac{A_{\text{epoxy,polymer}}}{A_{\text{ref,polymer}}}}{\frac{A_{\text{epoxy,monomer}}}{A_{\text{ref,monomer}}}}\right) \cdot 100\% \quad (1)$$

https://doi.org/10.1021/acsapm.2c01728
ACS Appl. Polym. Mater. 2023, 5, 731−742

where $A_{epoxy,polymer/monomer}$ is the area of the epoxy signal at 915 cm^{-1} in the polymer/monomer and $A_{ref,polymer/monomer}$ is the area of the reference band in the polymer/monomer.

Proton NMR Study. Formulations of around 1 g were composed as follows: difunctional epoxy monomers (ISE and DGEVA) were mixed in an equimolar ratio (in respect to reactive groups) with hexanediol and stirred in a heated aluminum block at 60 °C. One sample per formulation was prepared for proton NMR analysis by diluting the reaction mixture with ~0.5 mL of DMSO-d_6. Afterward, 1 wt % of the catalyst imidazole was added and stirring was continued at 60 °C. Every 30 min, a sample was prepared and analyzed by NMR spectroscopy. The conversion of epoxy and alcohol moieties was determined by following the decrease in epoxy and OH signal integrals over time, using eq 2

$$\text{conversion}\ [\%] = \left(1 - \frac{\text{integral}\ (t_x)}{\text{integral}\ (t_0)}\right) \cdot 100\% \tag{2}$$

where integral (t_x) is the area of the corresponding peaks at determined time points ($t = t_x$) and integral (t_0) is the area of the corresponding peaks at determined time points ($t = t_0$).

The rate of polymerization (R_p) was determined according to eq 3. Therefore, monomer conversion (%) was plotted against the reaction time (s) and the slope of the graph gave the rate of polymerization ($R_{p,s}$) in s^{-1}, which describes the conversion of the monomer per time (s). To obtain the rate of polymerization as the concentration ($mol \cdot L^{-1}$) per time (s), the density (ρ in $g \cdot L^{-1}$) and molecular mass ($g \cdot mol^{-1}$) of the monomer were used. The density of the monomers was determined by using a pycnometer with an exact volume of 1 mL, and the values are depicted in the Supporting Information in Table S3.

$$R_p\left[\frac{\text{mol}}{L \cdot s}\right] = \frac{R_{p,s}[1/s] \cdot \rho[g/L]}{M[g/mol]} \tag{3}$$

where R_p is the rate of polymerization [$mol \cdot L^{-1}\ s^{-1}$], $R_{p,s}$ is the rate of polymerization derived from the slope of conversion per time graph [s^{-1}], ρ is the density of the monomer at 60 °C [$g \cdot L^{-1}$], and M is the molecular weight of the monomer [$g \cdot mol^{-1}$].

Reactivity Study *via* DSC. About 10 mg (with an accuracy of ±0.1 mg) of each formulation was weighed in an aluminum pan and subsequently sealed with an aluminum lid. An empty pan was used as reference. The measurements were conducted on a simultaneous thermal analyzer (STA 449 F1 Jupiter, NETZSCH), and the temperature was raised from 25 to 200 °C with a heating rate of 5 K min^{-1}. For analysis of the DSC plots, the onset of the exothermal peak was evaluated by laying tangents and intersecting them. Heat of reaction was determined through the integration of heat flow over the exothermal peak. All measurements were conducted in duplicates, and the results were averaged.

Viscosity Measurements and Storage Stability. Viscosity measurements were conducted on a modular compact rheometer MCR 300 by Physica Anton Paar. Viscosity of the formulations was measured from 60 to 100 °C with a CP-25 measuring system (diameter 25 mm), a gap of 48 μm, and a constant shear rate of 100 s^{-1}. All measurements were conducted in triplicates, and the results were averaged. For the storage stability study, the formulations were stored at room temperature (25 °C) and viscosity measurements were conducted at predetermined time points (0, 1, 3, 5, 7, 10, 14, 21, and 28 days).

Dynamic Mechanical Thermal Analysis (DMTA). Dynamic mechanical thermal analysis (DMTA) measurements were performed with an Anton Paar MCR 301 with a CTD 450 oven and an SRF12 measuring system. The polymer specimens were tested in torsion mode with a frequency of 1 Hz and a strain of 0.1%. The temperature was increased from −100 to 200 °C with a heating rate of 2 °C min^{-1}. The storage modulus (G') and loss factor (tan δ) curves were processed with the software Rheoplus/32 V3.40 from Anton Paar. The glass transition temperature (T_G) was obtained from the maximum of the loss factor (tan δ_{max}). Additionally, G' at the rubbery plateau (G'_r) and full width at half maximum (FWHM) of tan δ_{max} were determined.

G'_r was used to calculate the average mesh size L of the networks as a measure for the cross-linking density of polymer networks in eq 4.[34]

$$L = \left(\frac{R \cdot T}{G'_r \cdot N_A}\right)^{1/3} \tag{4}$$

where L is the average mesh size [nm], R is the molar gas constant [$J\ K^{-1}\ mol^{-1}$], T is the temperature at which G'_r was determined (T_G + 30 °C)[K], G'_r is the storage modulus at the rubbery plateau [Pa], and N_A is the Avogadro number [mol^{-1}].

Tensile Test. Tensile tests were performed on a Zwick Z050 tensile machine, which reaches a maximum test force of 50 kN. The samples were strained with a crosshead speed of 5 mm min^{-1} and a maximum force of 1 kN. During the measurement, a stress−strain plot was recorded for analysis. Six specimens were tested per formulation with satisfactory reproducibility.

RESULTS AND DISCUSSION

Monomer Synthesis. The synthesis of epoxy resins is a well-known industrial process involving the condensation of phenols with an excess of epichlorohydrin and a strong base such as NaOH. Unfortunately, the structure and molecular weight of the resulting epoxy monomers are strongly dependent on the stoichiometry of the reactants. To minimize the formation of higher molecular weight oligomers, reactions are carried out with an excess of epichlorohydrin and upon the addition of a phase-transfer catalyst to assist the phenolate anion into the organic phase. Furthermore, epichlorohydrin acts as the reactive solvent, eliminating the need for additional solvents and the excess can be recovered *via* distillation after the synthesis. The aromatic monomer DGEVA was synthesized from the corresponding phenolic compound vanillyl alcohol as reported previously by Fache *et al.*[27] PHTE was prepared in a modified protocol from Guzmán *et al.* starting from the bio-derived trifunctional phenol phloroglucinol.[31] Herein, the phenolic compounds were treated with an excess of epichlorohydrin and an aqueous sodium hydroxide solution with tetrabutylammonium chloride as the phase transfer catalyst to obtain DGEVA in a yield of 82% and PHTE in 56% yield after purification by column chromatography on silica gel.

Conversion of aliphatic alcohols into glycidyl ethers requires altered synthesis routes. The reaction of such compounds with epichlorohydrin leads to the formation of secondary alcohols with similar pK_a values that are able to react with another epoxy group of epichlorohydrin, resulting in homopolymerization and a mixture of epoxy monomers and chlorohydrins as the final product. Therefore, for the synthesis of the cycloaliphatic monomer ISE, a two-step procedure that was reported by Chrysanthos *et al.* was used.[26] In the first step, isosorbide was reacted with allyl bromide and thereafter the double bonds were oxidized using *m*-CPBA to give the target compound in 65% yield after purification *via* column chromatography.

Polyaddition Catalyst Screening. Foix *et al.* showed that the reaction of epoxy and alcohol monomers requires tertiary amines as catalysts.[16] Therefore, a selection of commercially available tertiary amines (Scheme 2b) was tested regarding their efficiency to catalyze the epoxy-alcohol polyaddition. The curing process was investigated using TMPTG as the epoxy monomer and trimethylolpropane (TMP) as the alcohol component. The FT-IR spectra of the TMPTG/TMP system

https://doi.org/10.1021/acsapm.2c01728
ACS Appl. Polym. Mater. 2023, 5, 731−742

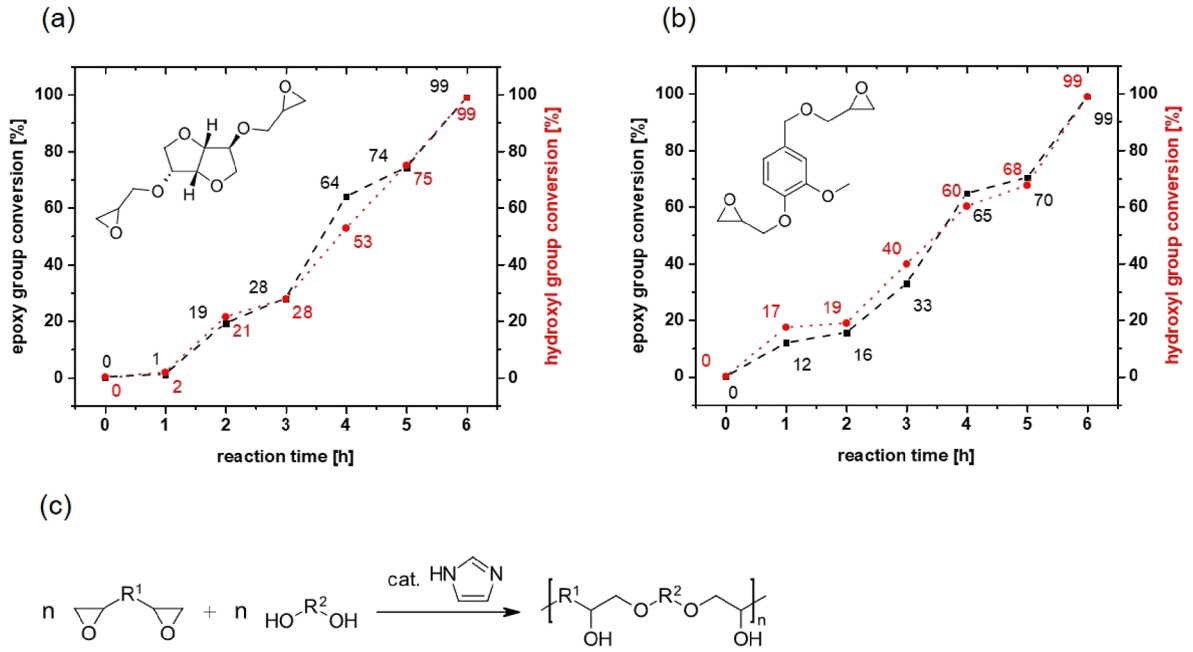

Figure 1. Conversion of epoxy groups (black square) of ISE (a) and DEGVA (b) and hydroxyl groups (red circles) of hexanediol in the bulk polymerization (60 °C) using 1 wt % of imidazole as the catalyst. For better visibility, the symbols were connected with straight lines. (c) Proposed general scheme of the polyaddition between difunctional epoxy and alcohol monomers giving poly(ether-alcohols).

were recorded prior and after thermal polymerization to assess the process of the curing reaction. In the first study, 5 wt % of each catalyst were added to the monomer system and the formulations were cured. Figure S1 (Supporting Information) shows that tertiary amines enable the polymerization of epoxides and alcohols, represented by a decrease in the absorption peak of the epoxy signal at 910 cm^{-1}.

As can be seen in Table S1 (Supporting Information), the addition of 5 wt % of TEA and DMA to the epoxy/alcohol system leads to low epoxy group conversions (<15%), while adding non-nucleophilic bases (TMG and DBN) increased the total epoxy group conversion to 25%. The different catalytic efficiency of the amines can be attributed to their different nucleophilicity and pK_a values: aliphatic amines (e.g., TEA) are stronger bases than aromatic amines (e.g., DMA). The formed alkyl ammonium ion is more stable than the corresponding aryl ammonium ion as the positive charge can be delocalized on the benzene ring, lowering the basicity of aromatic amines. Hence, TEA acted as a better catalyst than DMA. TMG and DBN represent a class of non-nucleophilic bases with a pK_a ∼13. Due to their strong base character, epoxy group conversion was enhanced (25%) compared to the previously discussed amines. Among the screened tertiary amines, imidazoles IM and 1MIM performed best as a full epoxy group conversion (>90%) was achieved.

As a result of the best catalytic efficiency, the unsubstituted imidazole IM was further investigated. The amount of catalyst was varied from 0.1 to 10 wt % (Supporting information, Table S2) in formulations containing TMPTG and TMP, revealing that 1−10 wt % of imidazole successfully catalyzed the epoxy-alcohol reaction. Furthermore, decreasing the catalyst amount to 0.1 wt % resulted in no conversion of epoxy moieties. Therefore, it was decided to use 1 wt % of imidazole as the catalyst for further studies.

Proton NMR Study on the Polyaddition Reaction. For the model study on the polymerization mode of epoxy-alcohol polyaddition, ^{1}H-NMR spectroscopy was chosen. Difunctional epoxy monomers ISE and DGEVA were polymerized in bulk with hexanediol, ideally giving linear and soluble polymers *via* the attempted polyaddition reaction (Figure 1c). The progress of the reaction was followed by the decrease in the characteristic epoxy and −OH peaks in the NMR spectra (Figures S2−S5). Figure 1a shows the conversion of epoxy and −OH peaks for the isosorbide-derived monomer ISE. As can be seen in Figure 1a, epoxy group conversion (black dots) as well as the −OH group conversion (red circles) proceeded in a similar pace. Interestingly, the reaction exhibited an induction period of around 1 h, while after 6 h, full conversion of both monomers was reached. Hence, gathered data suggests that epoxy and hydroxyl monomers react exclusively with each other, giving polyaddition polymers and no significant anionic homopolymerization of the epoxy monomers is present.

Similar to the analysis of ISE, epoxy groups of DGEVA and hydroxyl groups of hexanediol (Figure 1b) react in a homogeneous way with one another. Interestingly, no induction period is visible and full conversion of both monomers was again reached after 6 h. Furthermore, the formation of secondary hydroxyl groups could be monitored for the monomer DGEVA (see the Supporting Information, Figure S5). Over time, a broad singlet peak at ∼5 ppm was detectable, indicating the possible presence of two hydroxyl groups. For the monomer ISE, such peaks were not detectable as the peaks of the heterocyclic isosorbide core (4.9−3.3. ppm) superpose the peaks of newly formed secondary alcohols (see the Supporting Information, Figure S4).

Finally, the rate of polymerization (R_p) was determined from the data obtained *via* the proton NMR study and is defined as the conversion of the monomers [mol L^{-1}] per time [s^{-1}] and is depicted in Table 1. From the slope of the conversion per time diagram (Figure 1a,b) and the density of the monomers at 60 °C (see the Supporting Information, Table S3), R_p was calculated. The monomer ISE showed an induction period of 1

https://doi.org/10.1021/acsapm.2c01728
ACS Appl. Polym. Mater. 2023, 5, 731−742

Table 1. Calculated Rate of Polymerization (R_p) of the Thermal Polymerization of Difunctional Epoxy Monomers ISE and DGEVA and the Difunctional Alcohol Hexanediol

	rate of polymerization [mmol L^{-1} s^{-1}]
ISE	24.0
DGEVA	24.1

h, after which the monomers started to react with hexanediol. Consequently, the rate of polymerization was determined at t = 1 h until full consumption of monomers. For DGEVA, no induction period was determined and R_p was calculated from t = 0 h on. The epoxy monomers ISE and DGEVA show a similar rate of polymerization of 24 mmol L^{-1} s^{-1}. Interestingly, functional group conversions of both monomers and consequently also the rate of polymerization show a rather linear behavior over time. Even though the reaction is conducted in bulk, one would expect a decrease in instantaneous reaction rate over time. One possible explanation for the observed zero-order kinetic is a decrease in reaction volume as the polymerization progresses. In bulk polymerization, the material is known to exhibit volumetric shrinkage as the reaction proceeds toward higher monomer consumption. During the polymerization, the bonds of the monomers are shortened from a van der Waals distance to a covalent bond distance, leading to shrinkage of the formed polymer.[38] Therefore, the apparent concentration of reactive groups is increased at any given time, resulting in the observed zero-order kinetic. Additionally, although we expected an ideal AA + BB step-growth polymerization, it has to be considered that the anionic homopolymerization of the epoxide monomers initiated by the imidazole cannot be ruled out completely. Consequently, if the anionic pathway still proceeded to some extent, then branched or cross-linked polymers may form, having a non-negligible impact on the polymer solubility. As can be seen in Figures S4 and S5, less soluble polymers lead to broadening of the NMR signals of the epoxide end-group that eventually can merge into the baseline and thus result in an overestimation of the functional group conversion based on integration of the relevant peaks.

Reactivity Study *via* DSC. After the evaluation of the polymerization mechanism *via* proton NMR, the reactivity of all monomers toward thermal polyaddition was studied *via* differential scanning calorimetry (DSC). The corresponding DSC thermograms are displayed in the Supporting Information, Figure S6. The following parameters were used to determine the reactivity of the monomers: first, the onset temperature (t_{onset}) gives information about the stability of the formulations. High onset temperatures lead to thermally more stable formulations and are therefore desirable. By contrast, low onset temperatures are displayed in highly reactive systems. Formulations containing aromatic monomers DGEVA and PHTE started to polymerize at around 90 °C with TMP and exhibit a peak maximum at around 110 °C (Table 2). By contrast, the onset temperatures of the formulations containing aliphatic monomers TMPTG and ISE were significantly higher with 118 and 114 °C, respectively. Additionally, the peak temperature of the aliphatic and cycloaliphatic monomers is around 20 °C higher (129 °C for TMPTG and 127 °C for ISE) compared to the phenol-derived epoxy monomer formulations. The presence of aromatic rings in the epoxy monomers DGEVA and PHTE enhances the reactivity by an inductive effect. Electron density is withdrawn from the epoxy moieties, thus making them more electrophilic, and base-catalyzed curing is facilitated at lower temperatures.

Additionally, by integration of the exothermic DSC peak, the heat of polymerization (ΔH) is obtained, and by comparison with the theoretical heat of polymerization (~100 kJ per mol epoxy for epoxy-amine polyadditions),[19,39,40] the epoxy conversion was calculated. High conversions of >90% were obtained for the aliphatic monomers TMPTG and ISE. By contrast, the aromatic monomers DGEVA (84%) and PHTE (73%) exhibited lower epoxy group conversions according to the heat of polymerization obtained *via* DSC measurements. High reactivity of these monomers (indicated by a lower t_{onset} of <95 °C) led to early gelation during polymerization, which hindered monomer mobility and resulted in low epoxy group conversion according to DSC.

For comparison, the epoxy group conversion was furthermore determined using FT-IR spectroscopy of the polymerized specimens after the DSC analysis and is depicted in Table 2. According to the IR spectra, all of the monomers polymerized with high conversions (≥85%), which confirms a fast and efficient polyaddition reaction between the epoxy monomers and trimethylolpropane. Interestingly, higher epoxy group conversions were calculated for the aromatic monomers DGEVA and PHTE. These deviations can be attributed to the fact that the value of the theoretical heat of polymerization of epoxy groups was used for the calculation of the epoxy group conversion and may differ depending on the monomer. Additionally, it has to be considered that the DSC specimens were heated up to 200 °C and thus beyond the exothermal DSC peak maximum, enabling post-curing of the samples that could increase the epoxy group conversion.

For further cross-validation of the previous results, the respective theoretical heats of polymerization were calculated from the derived values for the heat of polymerization (ΔH) and the determined epoxy group conversion in the FT-IR

Table 2. Onset Temperature, Peak Temperature, and Heat of Polymerization of Formulations Containing Epoxy Monomers TMPTG, ISE, DGEVA, PHTE, and TMP as the Alcohol Component[c]

	onset temperature [°C]	peak temperature [°C]	ΔH[J·g^{-1}]	conversion *via* DSC [%][a]	conversion *via* IR [%]	ΔH_0[kJ·mol^{-1}][b]
TMPTG	118 ± 4	129 ± 2	470 ± 1	98.5	>99	104
ISE	115 ± 2	127 ± 2	543 ± 6	94.7	98.2	105
DGEVA	94.3 ± 0.6	111 ± 1	490 ± 6	83.7	89.2	99.1
PHTE	91.1 ± 0.4	111 ± 1	516 ± 5	73.4	85.3	122

[a]Conversion *via* DSC was calculated by comparing the obtained ΔH values of each formulation with the theoretical heat of polymerization (100 kJ mol^{-1}).[39] [b]Theoretical heat of polymerization ΔH_0 of each monomer was calculated from the measured heat of polymerization (ΔH) and the epoxy group conversion *via* IR. [c]Conversion of epoxy groups was studied *via* DSC and FT-IR, and calculated heat of polymerization ΔH_0 is displayed. Equimolar ratios of functional groups were reacted with 1 wt % imidazole as the catalyst.

https://doi.org/10.1021/acsapm.2c01728
ACS Appl. Polym. Mater. 2023, 5, 731−742

spectra (Table 2). The monomers TMPTG, ISE, and DGEVA show similar ΔH_0 of ~99 to 105 kJ (mol epoxy)$^{-1}$, which is in good correlation with the theoretical value for the epoxy functionality reported in literature (ΔH_0 ~100 kJ (mol epoxy)$^{-1}$).[39] Interestingly, for the trifunctional monomer PHTE, the highest ΔH_0 of 122 kJ (mol epoxy)$^{-1}$ was obtained, which is in correspondence to the previously discussed high reactivity of the monomer.

Storage Stability of the Formulations. The intrinsic high reactivity of tertiary amines toward epoxides limits their storage stability. Therefore, improving the thermal stability of such formulations is necessary to facilitate the use in industry. The storage stability of epoxy monomers and TMP in equimolar ratios and 1 wt % of the catalyst imidazole was investigated *via* rheology measurements at room temperature (Figure 2). Viscosity measurements were conducted at 60 °C

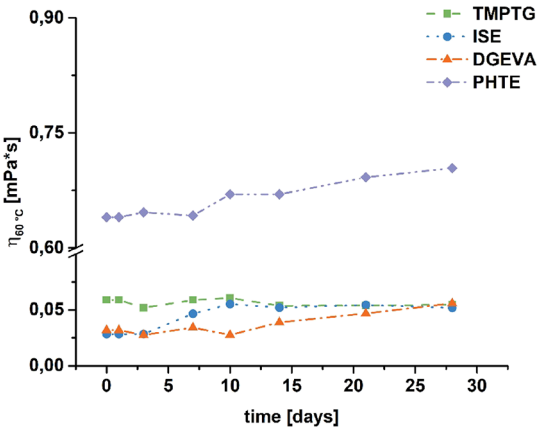

Figure 2. Viscosity at 60 °C over time (days) for formulations containing 50 mol % TMPTG, ISE, DGEVA, and PHTE as epoxy monomers and 50 mol % TMP as alcohol. Formulations were stored at room temperature (25 °C) over 30 days.

to ensure good miscibility of all components since the solid epoxy monomers DGEVA and PHTE partially recrystallized over time. The formulations show no significant increase in viscosity for the first 7 days. A slight increase in viscosity for ISE is observed after approximately 10 days (46.6−52.2 mPa·s), where the viscosity does not increase significantly at longer times, reaching a viscosity of 51.9 mPa·s after 28 days. For DGEVA, a marginal increase in viscosity is exhibited after 14 days (38.9−46.9 mPa·s), where TMPTG and PHTE show no significant increase in viscosity over 28 days, indicating sufficient storage stability at room temperature.

Thermomechanical Properties of Cross-Linked Networks. The final thermomechanical properties of polymer networks are affected by the underlying network architecture and can be characterized using dynamic mechanical thermal analysis (DMTA). DMTA provides the impact of the monomer structure on the thermomechanical properties of polymer networks. The method is used to obtain the storage modulus (G'), loss modulus (G''), and the loss factor (tan δ) at different temperatures. The macroscopic glass transition (T_G) is associated with the loss factor and is dependent on various physicochemical and mechanical factors.[41] Moreover, the storage modulus at the rubbery plateau G'_r (measured at T_G + 30 °C) is an indication for the cross-linking density. Hence, high G'_r values correlate with a high cross-linking density of the polymers.[42]

Prior to DMTA measurements, the epoxy group conversion of the polymers was determined using FT-IR, revealing that the epoxy peak in the IR spectra (910 cm^{-1}) completely disappeared for all polymers.

Figure 3a depicts the storage modulus G', and Figure 3b depicts the loss factor tan δ of polyadducts containing TMPTG, ISE, DGEVA, and PHTE as epoxy monomers and TMP as the hydroxyl component. For the rest of this study, the polymers will simply be called poly(epoxy monomer), although the polyadduct with TMP is discussed. Furthermore, Table 3 summarizes relevant results (T_G, G'_r, and FWHM) of the analysis. Poly(TMPTG) exhibits a sharp maximum in the loss factor at 2 °C, which is well below room temperature. By contrast, the more rigid cycloaliphatic core of ISE leads to an enhanced glass transition temperature for poly(ISE) (48 °C) and G'_r to 23.4 MPa, stemming from the bulky linker of the monomer and giving almost no degrees of rotational freedom. It was previously shown for aliphatic and aromatic polyesters that the cyclic structure of isosorbide provides more rigidity than standardly used diols such as butane diol.[43] The aromatic backbone of poly(DGEVA) is known to increase the rigidity of polymers,[44] leading to a T_G of 35 °C, although G'_r (1.85 MPa) was decreased compared to the ISE-based polymer. The linker of poly(DGEVA) is asymmetrical with different degrees of rotational freedom of bonding to the glycidyl groups, leading to a lower G' in the rubbery plateau. As a result of the trifunctional nature of PHTE and possible π-stacking, highly cross-linked poly(PHTE) shows the highest glass transition temperature (104 °C) and G'_r (39.9 MPa) of all specimens.

The shape of tan δ corresponds to the network structure, where the width and breadth of the peak provide information on the degree of homogeneity of the material.[45] Overall, sharp glass transitions were observed for the polyadducts, recognizable by low FWHM of the tan δ peak maximum. FWHM of the tan δ peak is around 18 °C for poly(TMPTG) and poly(DGEVA) and slightly increased for poly(ISE) (21 °C) and poly(PHTE) (32 °C). Hence, low FWHM values imply the formation of very homogeneous polymer networks. Cross-linking density of polymer networks is related to the amplitude of the loss factor tan δ: the lower the amplitude, the more rigid and cross-linked is the corresponding material.[41] Comparison of the peak height clearly outlines the impact of aromatic and bicyclic linkers on the properties of the polymers. While the aliphatic chains in poly(TMPTG) provide flexibility, introducing the bulky core of isosorbide and aromatic moieties of vanillyl alcohol and phloroglucinol results in a significant reduction of the amplitude of tan δ, indicating higher rigidity and thus cross-linking density. These observations are in correspondence with the previously mentioned G'_r values. While the aliphatic and thus flexible poly(TMPTG) network shows G' at the rubbery plateau of 0.51 MPa, G'_r of poly(PHTE) is increased by 750% to 39.9 MPa, indicating both higher rigidity and cross-linking density. The same conclusion is drawn for poly(ISE) as it shows a G'_r increase of 500% compared to the aliphatic polymer. Another parameter that is closely related to the cross-linking density of polymers is the average mesh size L. Highly cross-linked materials exhibit lower mesh sizes, whereas bigger average mesh sizes are associated with looser cross-linked networks (Table 3).[34] Indeed, calculated values agree with G'_r values and the observations from the amplitude of G'_r:poly(TMPTG) show the highest tan δ amplitude and lowest G'_r value, which correspond with the highest average mesh size of 2.02 nm and

https://doi.org/10.1021/acsapm.2c01728
ACS Appl. Polym. Mater. 2023, 5, 731−742

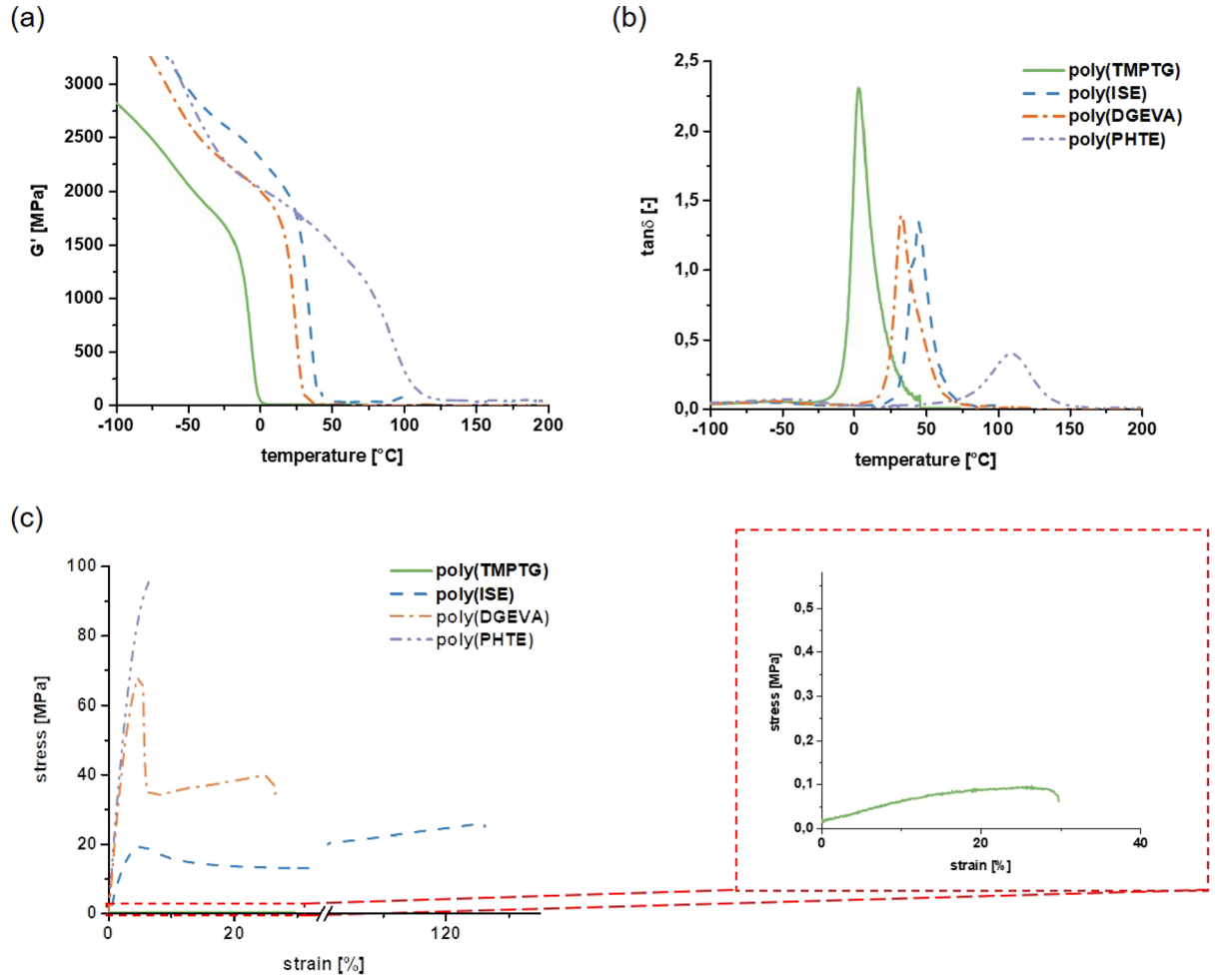

Figure 3. (a) Storage modulus (G') and (b) loss factor (tan δ) of polyadducts containing TMP as the alcohol monomer and TMPTG (green solid), ISE (blue dashed), DGEVA (orange dash-dot), and PHTE (purple dash dot-dot) as epoxy monomers. (c) Representative stress−strain diagram of tensile tests of the polyadducts. A magnification of the stress−strain plot of poly(TMPTG) is presented. Polyaddition of epoxy monomers and TMP as the alcohol component (equimolar ratio of functional groups) for (thermo)mechanical tests was conducted using 1 wt % of imidazole as the catalyst at 90 °C over 18 h.

Table 3. Summarized Results of (Thermo)Mechanical Tests[a]

	T_G [°C]	FWHM of tan δ [°C]	G'_r [MPa]	L [nm]	σ_M [MPa]	ε_B [%]	U_T[MJ/m^3]
poly(TMPTG)	2	17.2	0.513	2.02	0.09 ± 0.03	29.9 ± 6.2	0.03 ± 0.01
poly(ISE)	48	20.6	23.4	0.592	21.0 ± 3.0	126 ± 5	17.7 ± 1.9
poly(DGEVA)	35	18.8	1.85	1.36	66.9 ± 2.7	27.3 ± 2.8	10.0 ± 1.3
poly(PHTE)	104	32.7	39.9	0.520	91.0 ± 7.2	7.20 ± 0.71	3.96 ± 0.41

[a]Polyadditions were conducted with 1 wt % of imidazole as the catalyst in bulk at 90 °C for 18 h. Equimolar ratios of epoxy and alcohol groups were used. T_G, FWHM, and G'_r of thermally cured epoxy:alcohol polyadducts poly(TMPTG), poly(ISE), poly(DGEVA), and poly(PHTE) were obtained *via* DMTA. The average mesh size L of the materials was calculated from eq 4. Average σ_M, ε_B, and U_T values for polyaddition polymers were calculated from tensile test measurements.

consequently lowest cross-linking density. Although poly(DGEVA) and poly(ISE) show similar tan δ heights, G'_r of the vanillin-derived DGEVA (1.85 MPa) is significantly lower than G'_r of poly(ISE) (23.4 MPa). Hence, the unsymmetrical nature of the DGEVA monomer and the different glycidyl ether groups (phenolic and benzylic) lead to networks with a bigger average mesh size (1.36 nm) and thus lower cross-linking density compared to poly(ISE) (L = 0.59 nm). Finally, polymers derived from the trifunctional monomer PHTE show both the highest G'_r and lowest average mesh size (0.52 nm) that concur with the previously discussed lowest tan δ as an indicator for the highest cross-linking density of all materials.

Tensile Tests of Cross-Linked Networks. To complete the study on the thermomechanical properties, tensile tests of the polyaddition polymers were conducted. DMTA analysis indicated the formation of homogeneous polymer networks that can be seen by sharp glass transitions. Therefore, tensile tests were measured to determine the influence of more homogeneous polymer networks on the mechanical properties. Table 3 summarizes the results of the analysis. High reproducibility of the method is presented by low standard deviations, and therefore, representative stress−strain diagrams for each polymer are depicted in Figure 3c.

https://doi.org/10.1021/acsapm.2c01728
ACS Appl. Polym. Mater. 2023, 5, 731−742

Poly(PHTE) exhibited the highest maximum tensile strength with 90 MPa, while poly(DGEVA) reached lower values of around 67 MPa. Interestingly, the polymers that were produced from the aromatic diglycidyl ether monomer DGEVA displayed a distinct yield point after reaching σ_M and increased elongation at break (27%) was observed. By comparison, poly(PHTE) showed a significantly decreased ε_B of around 7% as a result of the higher cross-linking density resulting from the trifunctional nature of the epoxy and hydroxyl monomer. Polymers derived from the aliphatic TMPTG displayed pronounced elastomer-like behavior, displayed by low σ_M (0.1 MPa) and high ε_B (30%) stemming from flexible aliphatic chains of both epoxy and hydroxyl monomers. Considering a low T_G of 2 °C, this behavior was expected as the tensile tests were conducted in the rubbery state of the polymers. Compared to the aromatic polymers, poly(ISE) displayed decreased maximum tensile stress (21 MPa) but higher elongation at break (125%). By that, it was shown that the aromatic backbones of poly(DGEVA) and poly(PHTE) contribute to the mechanical properties of the materials *via* π-stacking between the polymer chains. Strong and tough polymers were obtained compared to the rather elastic ISE-derived poly(ISE). Tensile tests showed that the cycloaliphatic core of the ISE monomer did not deliver as much strength to the polymers as an aromatic backbone.

Moreover, by integration of the tensile stress−strain plots, tensile toughness was calculated. Thermal polyaddition of ISE and TMP results in polymers with the highest tensile toughness (17.7 MJ m^{-3}) as a result of the high elongation at break of these specimens. Polymers derived from DGEVA exhibit a tensile toughness of 10 MJ m^{-3} followed by specimens containing PHTE (U_T ∼4 MJ m^{-3}). As expected, the elastomeric poly(TMPTG) displayed the lowest tensile toughness (<0.1 MJ m^{-3}) of all materials.

CONCLUSIONS

To conclude, it was shown in a proton NMR study that the functional groups of alcohol and epoxy monomers convert homogeneously over time upon addition of 1 wt % of an imidazole catalyst. The rate of polymerization for vanillyl alcohol and isosorbide-derived epoxy monomers with hexanediol was calculated to be 24 mmol L^{-1} s^{-1}. Additionally, thermal reactivity of all multifunctional monomers (TMPTG, ISE, DGEVA, and PHTE with TMP) was studied *via* DSC and all tested formulations showed high reactivity, with onset temperatures ranging from 90 to 120 °C and peak temperatures of about 110−130 °C. Furthermore, theoretical heat of polymerization was calculated for the polyaddition reaction and ranged from 90 kJ mol^{-1} for TMPTG, ISE, and DGEVA to 122 kJ mol^{-1} for PHTE-derived polymers. Additionally, the high storage stability of at least 1 month at ambient temperatures of the tested formualtions enables long-term and easy-to-handle use of premixed mixtures for industrial applications.

At the same time, this study provides information on bulk-polymerized polymer networks. By the implementation of a step-wise polyaddition, more homogeneous polymer networks were obtained that showed narrow glass transitions in DMTA measurements with FWHM of the tan δ ranging from 17 to 30 °C. Furthermore, by the variation of the monomer structure, T_G of the polymers could be tailored over a broad temperature range (from 2 °C for the flexible aliphatic poly(TMPTG) to more than 100 °C for the rigid poly(PHTE)). High chain flexibility of the aliphatic monomers TMPTG and ISE resulted in elastomer-like materials during tensile testing with high elonagtions at break (up to 130%), while the aromatic backbone in DGEVA- and PHTE-based materials led to materials of high tensile strength (>65 MPa). Additionally, it was shown that *via* the proposed step-wise polyaddition mechanism, bio-based poly(ether) networks of high tensile toughness (up to 18 MJ m^{-3}) were obtained.

Following the performed analyses, we can conclude that, herein, polyadducts from sustainable and renewable resources with outstanding thermomechanical properties, especially high tensile toughness, were successfully designed and developed. The objective of proposing alterantives to the state-of-the-art BADGE monomer has been achieved by the development of both elastic, low-T_G and rigid, high-T_G epoxy networks and a feasible industrial manufacturing protocol. In particular, the high T_G network (>100 °C) derived from PHTE can be considered to replace fossil-based polymers in key sections such as coatings for automotive or naval industries.

ASSOCIATED CONTENT

Supporting Information

The Supporting Information is available free of charge at https://pubs.acs.org/doi/10.1021/acsapm.2c01728.

Additional experimental details on the catalyst screening procedure (reaction conditions and conversion and FT-IR spectra of uncured and cured specimens), proton NMR study of difunctional monomers (ISE, DGEVA, and hexanediol), and DSC thermograms of the polyaddition between multifunctional monomers (TMPTG, ISE, DGEVA, and PHTE with TMP) (PDF)

AUTHOR INFORMATION

Corresponding Author

Stefan Baudis − *Christian Doppler Laboratory for Advanced Polymers for Biomaterials and 3D Printing, Vienna 1060, Austria; Institute of Applied Synthetic Chemistry, Technische Universität Wien, Vienna 1060, Austria;* orcid.org/0000-0002-5390-0761; Email: stefan.baudis@tuwien.ac.at

Authors

Antonella Fantoni − *Christian Doppler Laboratory for Advanced Polymers for Biomaterials and 3D Printing, Vienna 1060, Austria; Institute of Applied Synthetic Chemistry, Technische Universität Wien, Vienna 1060, Austria*

Thomas Koch − *Institute of Materials Science and Technology, Technische Universität Wien, 1060 Vienna, Austria*

Robert Liska − *Institute of Applied Synthetic Chemistry, Technische Universität Wien, Vienna 1060, Austria*

Complete contact information is available at: https://pubs.acs.org/10.1021/acsapm.2c01728

Notes

The authors declare no competing financial interest.

ACKNOWLEDGMENTS

Funding by the Christian Doppler Research Association within the framework of the "Christian Doppler Laboratory for Advanced Polymers for Biomaterials and 3D Printing" and the financial support by the Austrian Federal Ministry for Digital

and Economic Affairs and the National Foundation for Research, Technology and Development are gratefully acknowledged. The authors acknowledge TU Wien Bibliothek for financial support through its Open Access Funding Programme.

REFERENCES

(1) Fried, J. R.*Polymer Science and Technology*; Pearson Education: US: 2003.
(2) Skeist, I.*Epoxy resins;*Reinhold Pub. Corp.: New York, 1959.
(3) Auvergne, R.; Caillol, S.; David, G.; Boutevin, B.; Pascault, J.-P. Biobased Thermosetting Epoxy: Present and Future. *Chem. Rev.* **2014**, *114*, 1082−1115.
(4) Ramon, E.; Sguazzo, C.; Moreira, P. A Review of Recent Research on Bio-Based Epoxy Systems for Engineering Applications and Potentialities in the Aviation Sector. *Aerospace* **2018**, *5*, 110.
(5) Paolillo, S.; Bose, R. K.; Santana, M. H.; Grande, A. M. Intrinsic Self-Healing Epoxies in Polymer Matrix Composites (PMCs) for Aerospace Applications. *Polymer* **2021**, *13*, 201.
(6) Ramsdale-Capper, R.; Foreman, J. P. Internal antiplasticisation in highly crosslinked amine cured multifunctional epoxy resins. *Polymer* **2018**, *146*, 321−330.
(7) Morancho, J. M.; Ramis, X.; Fernández-Francos, X.; Konuray, O.; Salla, J. M.; Serra, À. Dual curing of an epoxy resin with dicarboxylic acids. *J. Therm. Anal. Calorim.* **2020**, *142*, 607−615.
(8) Vyazovkin, S.; Sbirrazzuoli, N. Kinetic methods to study isothermal and nonisothermal epoxy-anhydride cure. *Macromol. Chem. Phys.* **1999**, *200*, 2294−2303.
(9) Han, S.; Kim, W. G.; Yoon, H. G.; Moon, T. J. Curing reaction of biphenyl epoxy resin with different phenolic functional hardeners. *J. Polym. Sci., Part A: Polym. Chem.* **1998**, *36*, 773−783.
(10) Stuparu, M. C.; Khan, A. Thiol-epoxy "click" chemistry: Application in preparation and postpolymerization modification of polymers. *J. Polym. Sci., Part A: Polym. Chem.* **2016**, *54*, 3057−3070.
(11) Vidil, T.; Tournilhac, F.; Musso, S.; Robisson, A.; Leibler, L. Control of reactions and network structures of epoxy thermosets. *Prog. Polym. Sci.* **2016**, *62*, 126−179.
(12) Kudo, K.; Fuse, S.; Furutani, M.; Arimitsu, K. Imidazole-type thermal latent curing agents with high miscibility for one-component epoxy thermosetting resins. *J. Polym. Sci., Part A: Polym. Chem.* **2016**, *54*, 2680−2688.
(13) Heise, M. S.; Martin, G. C. Curing mechanism and thermal properties of epoxy-imidazole systems. *Macromolecules* **1989**, *22*, 99−104.
(14) Heise, M. S.; Martin, G. C. Analysis of the cure kinetics of epoxy/imidazole resin systems. *J. Appl. Polym. Sci.* **1990**, *39*, 721−738.
(15) Ooi, S. K.; Cook, W. D.; Simon, G. P.; Such, C. H. DSC studies of the curing mechanisms and kinetics of DGEBA using imidazole curing agents. *Polymer* **2000**, *41*, 3639−3649.
(16) Foix, D.; Ramis, X.; Ferrando, F.; Serra, A. Improvement of epoxy thermosets using a thiol-ene based polyester hyperbranched polymer as modifier. *Polym. Int.* **2012**, *61*, 727−734.
(17) Fernández-Francos, X.; Konuray, A.-O.; Belmonte, A.; De la Flor, S.; Serra, À.; Ramis, X. Sequential curing of off-stoichiometric thiol−epoxy thermosets with a custom-tailored structure. *Polym. Chem.* **2016**, *7*, 2280−2290.
(18) Ding, X.-M.; Chen, L.; Guo, D.-M.; Liu, B.-W.; Luo, X.; Lei, Y.-F.; Zhong, H.-Y.; Wang, Y.-Z. Controlling Cross-Linking Networks with Different Imidazole Accelerators toward High-Performance Epoxidized Soybean Oil-Based Thermosets. *ACS Sustainable Chem. Eng.* **2021**, *9*, 3267−3277.
(19) Rozenberg, B. A. In Kinetics, thermodynamics and mechanism of reactions of epoxy oligomers with amines, *Epoxy Resins and Composites II, Berlin, Heidelberg, 1986//*; Dušek, K., Ed. Springer Berlin Heidelberg: Berlin, Heidelberg, 1986; pp. 113−165.
(20) Acebo, C.; Picardi, A.; Fernández-Francos, X.; De la Flor, S.; Ramis, X.; Serra, À. Effect of hydroxyl ended and end-capped multiarm star polymers on the curing process and mechanical characteristics of epoxy/anhydride thermosets. *Prog. Org. Coat.* **2014**, *77*, 1288−1298.
(21) Morell, M.; Foix, D.; Lederer, A.; Ramis, X.; Voit, B.; Serra, À. Synthesis of a new multiarm star polymer based on hyperbranched poly(styrene) core and poly(ε-caprolactone) arms and its use as reactive modifier of epoxy thermosets. *J. Polym. Sci., Part A: Polym. Chem.* **2011**, *49*, 4639−4649.
(22) McCoy, J. D.; Ancipink, W. B.; Maestas, S. R.; Draelos, L. R.; Devries, D. B.; Kropka, J. M. Reactions of DGEBA epoxy cured with diethanolamine: Isoconversional kinetics and implications to network structure. *Thermochim. Acta* **2019**, *671*, 149−160.
(23) Vandenberg, L. N.; Hauser, R.; Marcus, M.; Olea, N.; Welshons, W. V. Human exposure to bisphenol A (BPA). *Reprod. Toxicol.* **2007**, *24*, 139−177.
(24) Gandini, A. The irruption of polymers from renewable resources on the scene of macromolecular science and technology. *Green Chem.* **2011**, *13*, 1061−1083.
(25) Woelk, H. U. Stärke als Chemierohstoff — Möglichkeiten und Grenzen. *Starch - Stärke* **1981**, *33*, 397−408.
(26) Chrysanthos, M.; Galy, J.; Pascault, J.-P. Preparation and properties of bio-based epoxy networks derived from isosorbide diglycidyl ether. *Polymer* **2011**, *52*, 3611−3620.
(27) Fache, M.; Auvergne, R.; Boutevin, B.; Caillol, S. New vanillin-derived diepoxy monomers for the synthesis of biobased thermosets. *Eur. Polym. J.* **2015**, *67*, 527−538.
(28) Fache, M.; Boutevin, B.; Caillol, S. Vanillin Production from Lignin and Its Use as a Renewable Chemical. *ACS Sustainable Chem. Eng.* **2016**, *4*, 35−46.
(29) Hernandez, E. D.; Bassett, A. W.; Sadler, J. M.; La Scala, J. J.; Stanzione, J. F. Synthesis and Characterization of Bio-based Epoxy Resins Derived from Vanillyl Alcohol. *ACS Sustainable Chem. Eng.* **2016**, *4*, 4328−4339.
(30) Ménard, R.; Negrell, C.; Fache, M.; Ferry, L.; Sonnier, R.; David, G. From a bio-based phosphorus-containing epoxy monomer to fully bio-based flame-retardant thermosets. *RSC Adv.* **2015**, *5*, 70856−70867.
(31) Guzmán, D.; Santiago, D.; Serra, À.; Ferrando, F. Novel Bio-Based Epoxy Thermosets Based on Triglycidyl Phloroglucinol Prepared by Thiol-Epoxy Reaction. *Polymer* **2020**, *12*, 337.
(32) Theophile, T., *Infrared Spectroscopy: Materials Science, Engineering and Technology;*IntechOpen: 2012.
(33) Purut Koc, O.; Bekin Acar, S.; Uyar, T.; Tasdelen, M. A. In situ preparation of thermoset/clay nanocomposites via thiol-epoxy click chemistry. *Polym. Bull.* **2018**, *75*, 4901−4911.
(34) Wang, J.; Ugaz, V. M. Using in situ rheology to characterize the microstructure in photopolymerized polyacrylamide gels for DNA electrophoresis. *Electrophoresis* **2006**, *27*, 3349−3358.
(35) Li, Q.; Aili, D.; Savinell, R. F.; Jensen, J. O., Acid−Base Chemistry and Proton Conductivity. In *High Temperature Polymer Electrolyte Membrane Fuel Cells: Approaches, Status, and Perspectives*; Li, Q.; Aili, D.; Hjuler, H. A.; Jensen, J. O., Eds. Springer International Publishing: Cham, 2016; pp. 37−57.
(36) Kothandaraman, J.; Goeppert, A.; Czaun, M.; Olah, G. A.; Surya Prakash, G. K. CO2 capture by amines in aqueous media and its subsequent conversion to formate with reusable ruthenium and iron catalysts. *Green Chem.* **2016**, *18*, 5831−5838.
(37) Matyska, M. T.; Pesek, J. J.; Tong, S.; Sandoval, J. E. Adamantyl Modified Silica via Olefin Hydrosilation on a Hydride Intermediate. *J. Liq. Chromatogr. Relat. Technol.* **2003**, *26*, 1169−1196.
(38) Luck, R. M.; Sadhir, R. K.*Expanding Monomers - Synthesis, Characterization, and Applications;*CRC Press: 1992; Vol. *1*st, p 416.
(39) Brandrup, J., *Polymer Handbook*. 4 ed.; Wiley & Sons: New York, 1999.
(40) Barton, J. M. In The application of differential scanning calorimetry (DSC) to the study of epoxy resin curing reactions.*Epoxy Resins and Composites I, Berlin, Heidelberg, 1985//*; Springer Berlin Heidelberg: Berlin, Heidelberg, 1985; pp. 111−154.
(41) Kalogeras, I. M.; Hagg Lobland, H. The nature of the glassy state: Structure and glass transitions. *J. Mater. Educ.* **2012**, *34*, 69−94.

https://doi.org/10.1021/acsapm.2c01728
ACS Appl. Polym. Mater. 2023, 5, 731−742

(42) Gorsche, C.; Seidler, K.; Knaack, P.; Dorfinger, P.; Koch, T.; Stampfl, J.; Moszner, N.; Liska, R. Rapid formation of regulated methacrylate networks yielding tough materials for lithography-based 3D printing. *Polym. Chem.* **2016**, *7*, 2009−2014.
(43) Fenouillot, F.; Rousseau, A.; Colomines, G.; Saint-Loup, R.; Pascault, J. P. Polymers from renewable 1,4:3,6-dianhydrohexitols (isosorbide, isomannide and isoidide): A review. *Prog. Polym. Sci.* **2010**, *35*, 578−622.
(44) Ng, F.; Couture, G.; Philippe, C.; Boutevin, B.; Caillol, S. Bio-Based Aromatic Epoxy Monomers for Thermoset Materials. *Molecules* **2017**, *22*, 149.
(45) Terry, J. S.; Taylor, A. C. The properties and suitability of commercial bio-based epoxies for use in fiber-reinforced composites. *J. Appl. Polym. Sci.* **2021**, *138*, 50417.

https://doi.org/10.1021/acsapm.2c01728
ACS Appl. Polym. Mater. 2023, 5, 731−742